SUPPLEMENTARY MATERIAL

METHODS AND MATERIALS

Characterization of Stock Gold Nanoparticles

Electron Microscopy. TEM. A drop of GNPs in double-distilled water was placed on formvar-coated 400-mesh nickel grids and incubated for 10 minutes at room temperature. The solution was wicked off the grids using a piece of #1 Whatman paper, after which the grids were allowed to dry completely. Photomicrographs were taken at 100,000x magnification at 75 kV and compared to a catalase crystal imaged at the same magnification and accelerating voltage. **HRTEM**. Drops (5 – 10 µL) of GNPs in double–distilled water were placed on a carbon- and formvar-coated 400-mesh copper grid and the grids were allowed to dry completely. Photomicrogrpahs were taken at 700 k. DigitalMicrograph® analysis software (Gatan Inc., Pleasanton, CA, USA) was used to analyze the interplanar distances within the GNPs presented on each photomicrograph. **SEM.** Drops (5-10 µl) of GNPs were placed on a graphite-painted aluminum stub. The stub was placed on the holder and loaded into the instrument at an accelerating voltage of 10 kV.

Dynamic Light-Scattering Spectroscopy. Each 1-mL sample was transferred to a square cuvette to evaluate hydrodynamic particle size, and then transferred to a folded capillary cell for zeta potential measurements. In brief, 1mL of stock GNPs (in double-stilled water) was vortexed to promote a homogeneous solution. All sample measurements were acquired in triplicate at 25 ^{o}C.

X-ray Photoelectron Spectroscopy. High-collection efficiency was obtained by use of a magnetic immersion lens. The delay-line detector, comprising a multi-channel plate stack above a delay-line anode, was used for photoelectron detection. The instrument work function was calibrated to give a binding energy (BE) of 83.96 (0.05) eV (Mean [SD]) for the Au 4f7/2 line for metallic gold and the spectrometer dispersion was adjusted to give a BE of 932.62 (0.05) eV (Mean [SD]) for the Cu2p3/2 line of metallic copper. High-resolution analyses were carried out with an analysis area of 300 x 700 microns using a pass energy of 160 eV and with a step size of 0.5 eV. The samples experienced varying degrees of charging—

3.7 eV balance and 1 eV bias electrons were used to minimize this charging. Small pieces of silicon wafers were first ultrasonicated in deionized water (18.2MΩ) for 10 minutes to remove any debris from cutting the wafer and from adhering dust particles. The cleaned wafers were then boiled in Piranha solution (70:30 H_2SO_4:H_2O_2) for 10 minutes. The Piranha solution was cooled to room temperature before removing the wafers and each wafer was rinsed thoroughly with DI water (18.2 MΩ). The silicon wafers were dried under a stream of nitrogen and were cleaned by UV-ozone treatment for 30 minutes. This procedure removes any hydrocarbon contamination from the silicon wafer substrate and creates an extremely hydrophilic surface. The GNPs in solution were transferred to a re-circulated nitrogen atmosphere glove box (< 1 ppm O_2 and -80 ^oC dewpoint). The wafer was placed onto a clean copper XPS-sample stub. A small volume (~50 µl) of GNP sample solution was deposited onto the cleaned silicon wafer using a standard pipette. The solution was allowed to dry and the sample stub was transported into the XPS spectrometer vacuum for analysis.

Characterization of Gold Nanoparticles under Experimental Conditions

Pyrogene™ Recombinant Factor C (rFC) Endotoxin Detection Assay. Stock GNPs at concentrations of $1.43x10^3$, $1.43x10^6$, or $1.43x10^9$ GNPs/mL were added to DMEM/F12 50/50 medium containing supplements identical to that of our TEM and *ex-vivo* studies. Samples of culture medium that did not contain GNPs were included as negative controls. Duplicate samples were shipped at ambient temperature and stored at 2-8 ^oC upon arrival until performance of rFC assays. The rFC assay utilizes recombinant Factor C (rFC), an endotoxin-sensitive protein that is used in combination with a fluorogenic substrate to detect endotoxin in a solution via an incubating FLx800™ fluorescence microplate reader (BioTek Instruments, Inc., Winooski, VT, USA) equipped with WinKQCL® 4 Endotoxin Detection and Analysis Software (Lonza, Inc., Walkersville, MD, USA). Each assay was carried out in a 96-well plate and fluorescence was measured at time zero and after a one-hour incubation at 37°C ± 1°C using excitation/emission wavelengths of 380/440nm. The difference between the one-hour reading and the time-zero reading (ΔRFU) was corrected for blank ΔRFU fluorescence. The log net fluorescence was

proportional to the log endotoxin concentration and was linear in the 0.01 to 1.0 EU/mL range. The concentration of endotoxin in each sample was calculated relative to a standard curve.

TEM. Stock GNPs at concentrations of either $2.85x10^7$ or $2.85x10^{10}$ particles/mL medium (n= 3 samples) were exposed to culture conditions that were identical to those of our rat ovary culture experiments (see Ex-Vivo *Culture of Rat Ovary*) at four different time periods (0, 12, 24, and 48 hours) at 37°C in 5% CO_2 in air. These model concentrations were chosen due to pragmatic TEM considerations. DMEM/F12 50/50 medium was supplemented with 5% fetal calf serum, 50 µg/mL gentamycin, 50 ng/mL follicle-stimulating hormone (FSH) and $1x10^{-7}$ M androstenedione. After incubation, large protein aggregates were removed from the medium by centrifugation at 800 g for 30 sec. The nanoparticles were washed twice in double-distilled water (dd H_2O) by centrifugation at 1750 g for 10 min. Afterwards the nanoparticles were resuspended in 50 µl of dd H_2O. The entire resuspended pellet was allowed to air dry on carbon-coated, 400-mesh TEM grids.

DLS. At three different time points (12, 24, 48 hours), a 1-mL sample of culture solution was removed and prepared for evaluation of hydrodynamic diameter and zeta potential as described above. Non-incubated samples of supplemented culture medium without GNPs were also included in our analysis as negative controls.

Use of the *In-vitro* Sedimentation, Diffusion, and Dosimetry Model to Estimate Target-Tissue Dose. A computer simulation was conducted for GNPs at a concentration of 1.43×10^9 particles/mL using the following values that were specific to our *ex-vivo* system: 4.0 mm (medium height), 1.0 g/mL (medium density), 0.00074 Ns/m^2 (medium viscosity), 19.3 g/mL (particle density), 37 °C (temperature), 48 hours (maximal simulation time) and 10 nm (primary particle diameter). The computer simulation was conducted in the presence or absence of gravity (9.81 m/s^2) to evaluate the extent of gravitational influence on the transport of GNPs in our culture model due to the fact that each intact rat ovary was cultured on a nylon mesh oriented *above* either the negative control or the GNP-supplemented culture medium. This evaluation was absolutely critical for diffusion simulations such as ISDD because of the significant influence of

gravity on particle diffusion; results indicated, however, no significant effect of gravity on particle diffusion in our model. The estimated percentage of ovarian surface area relative to the surface area of the culture well had to be determined and factored into our ISDD results because the model solely predicts the dose of particles delivered to a monolayer of cells that is dispersed uniformly over the entire bottom of a culture well. Upon factoring in relative ovarian surface area (approximately 25% of the total well-surface area), results were divided by 1000 or 1 000 000 to determine the estimated target-tissue dose delivered to rat ovary as a function of time upon exposure to $1.43x10^6$ or $1.43x10^3$ particles/mL GNPs *ex vivo*, respectively.

Radioimmunoassay. Concentrations of immunoreactive (ir)-inhibin in culture medium samples were measured as previously performed in the laboratory of Dr. Gen Watanabe in Tokyo, Japan (Hamada et al. 1989)—using antisera against bovine inhibin (TNDH-1) and bovine 32-kDa inhibin for both iodination and standard, respectively. Assays for all target hormones were validated for rat by demonstrating parallelism between rat serum samples in serial dilution versus authentic standards.

Multiple-Reference Gene-Quantitative Real-Time RT-PCR (MRG-qPCR). RNA was precipitated by adding 1/10 volume (10 µl) of 2 M NaCl in DEPC-treated water and four sample volumes (400 µl) of 100% ethanol, followed by incubation at -20^{o}C overnight. Samples were centrifuged and the supernatant decanted. RNA pellets were rinsed twice with 1 mL of 75% ethanol and blotted on a Kim-Wipe®. The samples were then centrifuged to collect extra fluid. Excess ethanol was removed via a 2.0-µl micropipette and the RNA pellet was allowed to air-dry for 10-15 minutes. Upon drying, the pellet was resuspended in 40 µl RNAse-free water. cDNA synthesis was conducted using the AffinityScript® Multiple Temperature cDNA Synthesis Kit per manufacturer's protocol. MRG-qPCR was performed using a StepOne Plus real-time qPCR instrument (Life Technologies Corp., Carlsbad, CA, USA; 95^{0}C [9 minutes]; 95^{o}C [15 seconds], 51^{o}C [30 seconds], 72^{o}C [45 seconds] for 40 cycles; 95^{o}C [30 seconds], 55^{o}C [30 seconds], 95^{o}C [30 seconds]), *Power* SYBR® Green PCR Master Mix, and gene-specific primers (designed using Primer3 software) to quantify selected transcripts important to ovarian steroidogenesis and oxidative stress (**Table**

S1). The PCR efficiency for all selected primer pairs was assumed to be 100%. All qPCR reactions (10 µl) were carried out in triplicate. Gel electrophoresis and melting-curve analysis were employed to ensure that the specific gene products of expected size were amplified.

Table S1. Summary of validated reference and target genes selected for multiple reference gene-qPCR experiment.

Gene Symbol	Gene Product	Sense Primer	Antisense Primer	NCBI Accession Number
Reference Genes				
Zc3h15	zinc finger CCCH-type containing 15	AGGAAGTGTAACCGCTTTTCC	TGCTCACTTTTCAGGTCGTC	NM_001010963.1
Gapdh	glyceraldehyde-3-phosphate dehydrogenase	CTGAGGACCAGGTTGTCTCC	AGGGCCTCTCTCTTGCTCTC	NM_017008.3
Actb	β-actin	CAGTGCTGTCTGGTGGCA	CGCAGCTCAGTAACAGTCCG	NM_031144.2
Target Genes				
Cyp11a1	side-chain cleavage enzyme	CTGGTCAAAAGTCGCCAAC	ATTCTGTGTGTGCCGTTCTC	NM_017286.2
Star	steroidogenic acute regulatory protein	TGAGGCCCAGTGTTAAGGAC	GCCTCAGTTCTGTTTTCCTG	NM_031558.2
Hsd3b1	3β-hydroxysteroid dehydrogenase	ATGTGGTTCTGGGTGTTACC	TGTCATTGCTGAAGCCTTTG	NM_001007719.3
Cyp17a1	17α-hydroxylase/17, 20 lyase	GGAGGGTGATCCCAAGGTAG	AGGAGGAAGGAGGACCGTAG	NM_012753.1
Cyp19a1	aromatase	CTGCTTTGCGTCCTAACATC	CACTGACAGHGCACAGTTTCC	NM_017085.2
Hmox1	heme oxygenase (decycling) 1	CAAAGACCAGAGTCCCTCAC	GGCAAGATTCTCCCCTGC	NM_012580.2
Sod2	superoxide dismutase 2, mitochondrial	GATTGCCGCCTGCTCTAA	CTACAAAACACCCACCACGG	NM_017051.2

Table S2. Summary of DLS analyses of GNPs under both stock and culture conditions.

Dispersant	Concentration (GNPs/mL)	Zeta Potential (mv)	Z-Average Diameter (nm)	PdI	pH
Double-distilled water	5.70×10^{12}	-24.4 (2.16) *(N=2, n=6)*	243.7 (122.8)	0.62 (0.14)	7.0
Culture Solution	0	-9.5 (0.99) *(N=2, n=6)*	46.1 (4.78)	0.73 (0.053)	7.1
	1.43×10^3	-9.0 (0.88) *(N=9, n=27)*	37.1 (7.63)	0.86 (0.18)	7.1
	1.43×10^6	-8.9 (0.61) *(N=8, n=24)*	37.0 (7.63) *(N=9, n=26)*	0.84 (0.17)	7.1
	1.43×10^9	-9.4 (0.73) *(N=9, n=27)*	37.0 (8.56) *(N=9, n=26)*	0.85 (0.17)	7.1

PdI= polydispersity index. The data were pooled for each specified concentration, independent of incubation period. Measurements of each sample were taken in triplicate. Values are presented as *MEAN (SD)*. *N* = number of replicate samples; *n* = number of total measurements acquired from N samples.

Table S3. Evaluation of the primary diameter of GNPs under experimental conditions using TEM.

Concentration (particles/mL)	Time (Hours) 0	12	24	48	Pooled
$2.85x10^7$					
Mean (nm)	10.6 (7.0)	10.0 (5.9)	9.2 (5.7)	9.3 (5.1)	9.8 (5.9)
Range (nm)	4.0 - 34.8	2.6 - 37.4	3.4 - 41.8	2.8 - 43.5	2.8 - 43.5
n	100	130	130	130	501
$2.85x10^{10}$					
Mean (nm)	7.5 (3.8)	9.4 (4.8)	10.3 (5.0)	11.0 (6.6)	9.3 (5.1)
Range (nm)	2.7 - 31.6	4.2 - 27.2	3.8 - 30.5	3.3 - 32.1	2.7 - 32.1
n	122	59	120	59	360
$Pooled_{(Overall)}$					
Mean (nm)					9.6 (5.5)
Range (nm)					2.7 - 43.5
n					861

Values are presented as *MEAN (SD)*. Data were pooled for each particle concentration, independent of incubation period (*Pooled, right*); and data were pooled independent of particle concentration and incubation period (*Pooled [Overall], bottom left*). n = number of particles measured.

Table S4. Summary of the elemental composition of the stock GNP surface as detected by XPS.

Type	Transition	Atomic Percent (%)
Oxygen (O)	1s	45.9
Carbon (C)	1s	27.9
Sodium (Na)	1s	17.7
Chloride (Cl)	2p	3.5
Silicon (Si)	2p	3.3
Potassium (K)	2p	1.7

Table S5. Summary of endotoxin contamination as a function of gold concentration in samples of supplemented culture medium.

Mixture	Mean Concentration of Endotoxin (ng/mL)
Culture Solution	1.55
$1.43x10^3$	0.53
$1.43x10^6$	0.72
$1.43x10^9$	1.43
Pooled $_{(GNPs)}$	0.89 (0.61)
range	0.476-2.11
n	6 samples
Pooled $_{(Overall)}$	1.06 (0.70)
range	0.476-2.24
n	8 samples

The mean value determined from duplicate samples is presented unless otherwise indicated. 0.01 ng/mL = 1.0 EU/mL endotoxin. Pooled $_{(GNPs)}$ = data were pooled for samples containing GNPs independent of concentration. Pooled $_{(Overall)}$ = all data were pooled regardless if GNPs were absent or present. Pooled data are presented as *MEAN (SD)*.

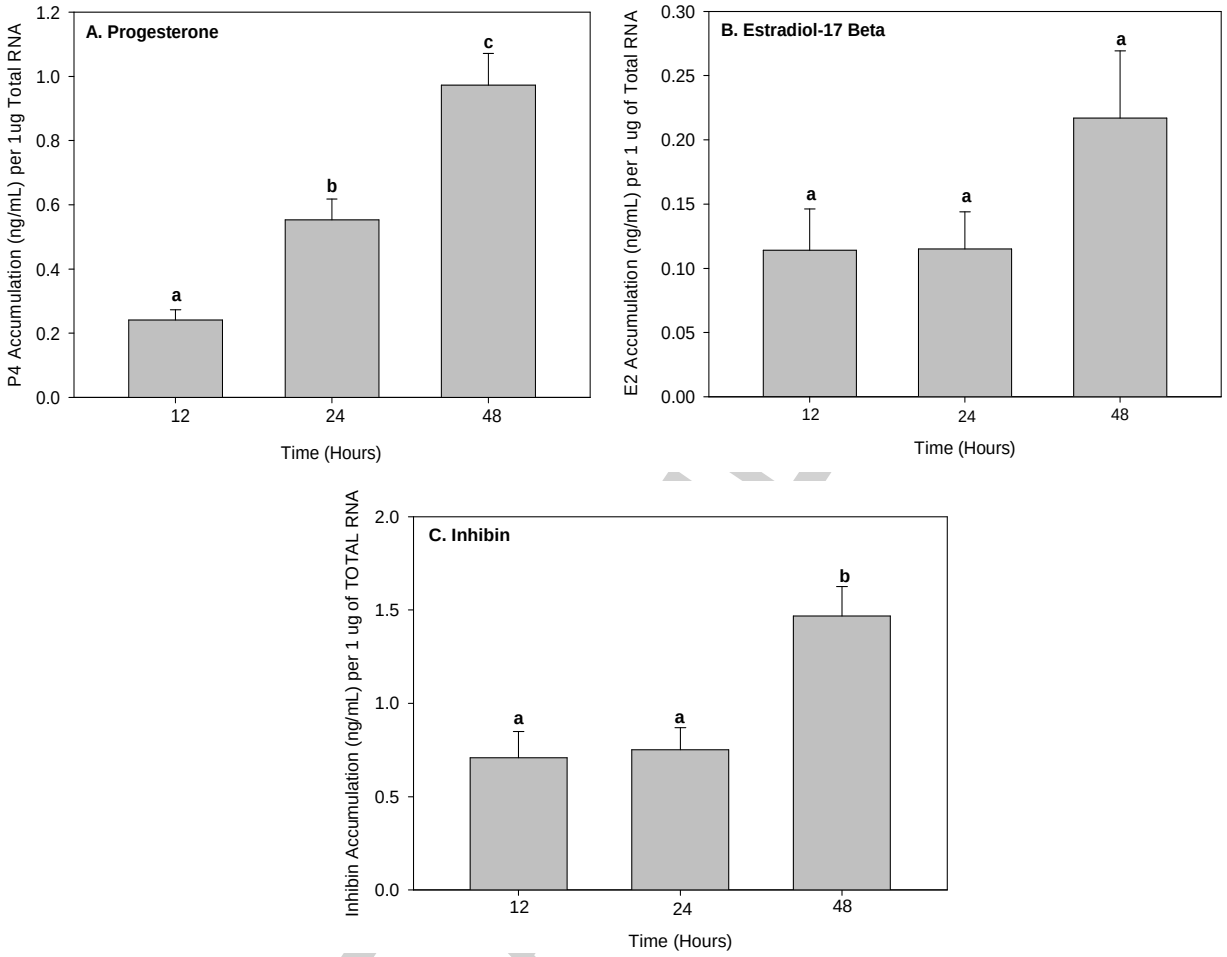

Figure S1. Analysis of (A) progesterone (P4), (B) estradiol-17β (E2), and (C) inhibin accumulation secreted from control rat ovaries as a function of time. (A) One-way ANOVA and Tukey's multiple-comparison test revealed a statistically significant time-dependent increase in P4 accumulation *ex vivo* (df= 83 rats, $p<0.001$). (B) One-way ANOVA showed no significant difference in E2 accumulation as a function of incubation period (df= 68 rats, $p= 0.159$). (C) One-way ANOVA and Tukey's multiple-comparison test revealed a statistically significant increase in inhibin accumulation after 48 hours of incubation compared to that of 12 and 24

hours (df= 78 rats, $p<0.001$). [a, b, c] Differing subscripts represent statistically significant differences among groups.

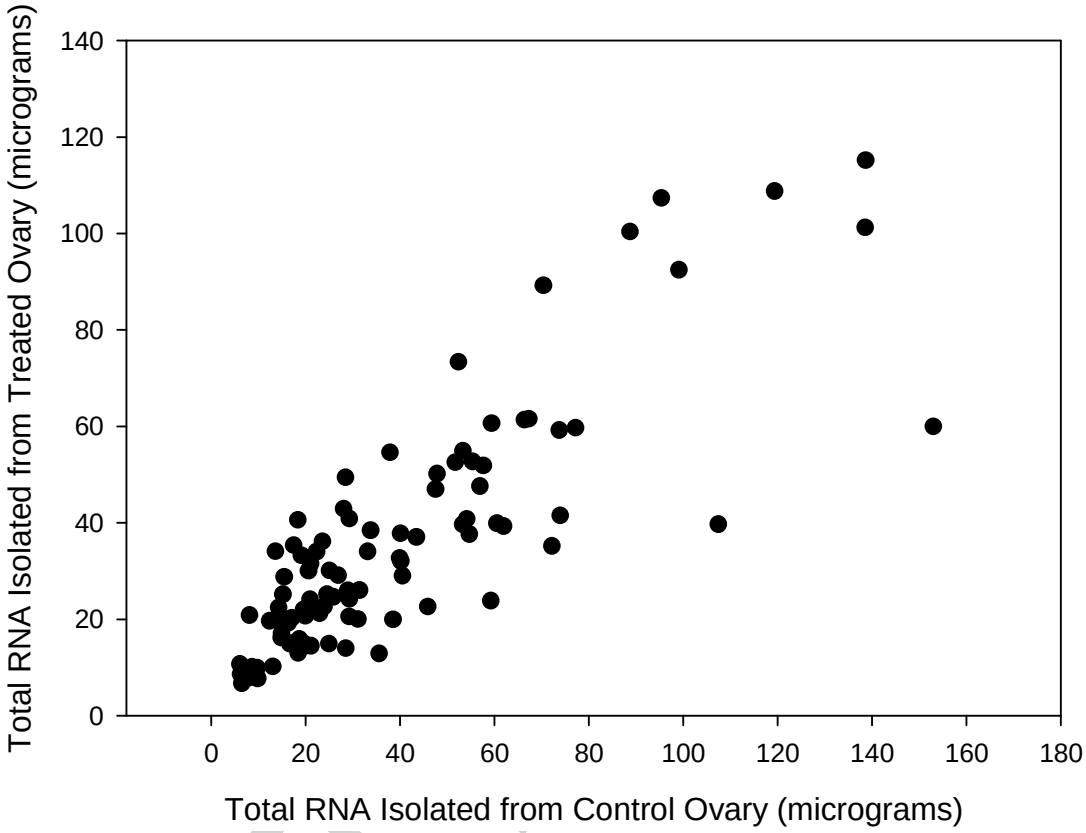

Figure S2. Analysis of the relationship between the total RNA isolated from control ovary and the total RNA isolated from the GNP-treated ovary of each respective ovary pair independent of incubation time and particle concentration. Pearson correlation showed a significant positive correlation between these two variables ($r= 0.836$, $p= 2.94x10^{-26}$, $n= 96$ rats).

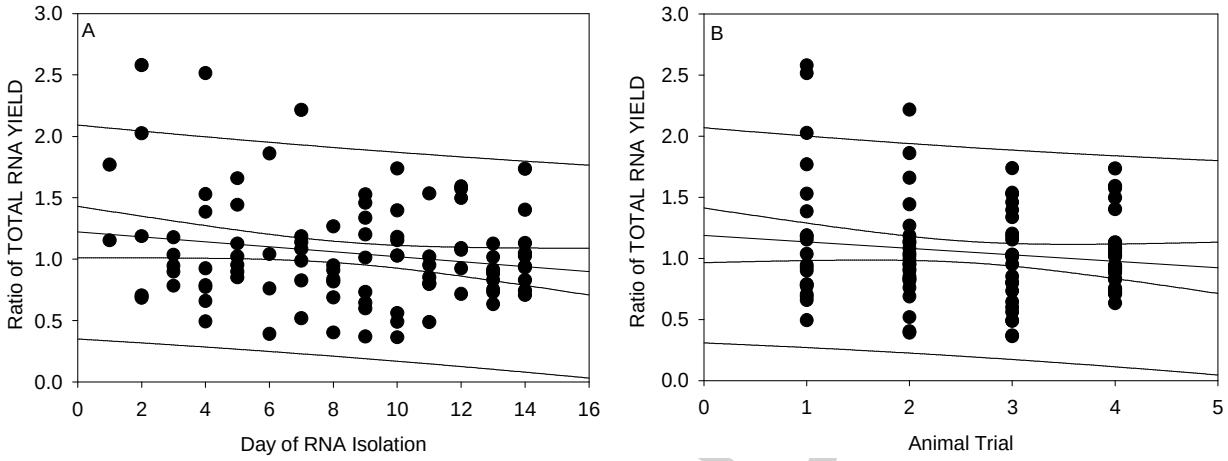

Figure S3. Effect of time (A) and animal trial (B) on RNA yield. (A) Simple linear regression showed no significant effect of time on total RNA yield ratio (treated ovary/control ovary) from each respective animal (df= 95 rats, $p>0.05$, $r^2= 0.0323$, adjusted [adj.] $r^2= 0.0220$; regression equation [reg eq]: $y= -0.0201x + 1.221$). (B) Simple linear regression also showed no statistically significant relationship between total RNA yield ratios and animal trial (df= 95 rats, $p>0.05$, $r^2= 0.0185$, adj. $r^2= 0.00801$; regression equation: $y= -0.0531x + 1.188$).

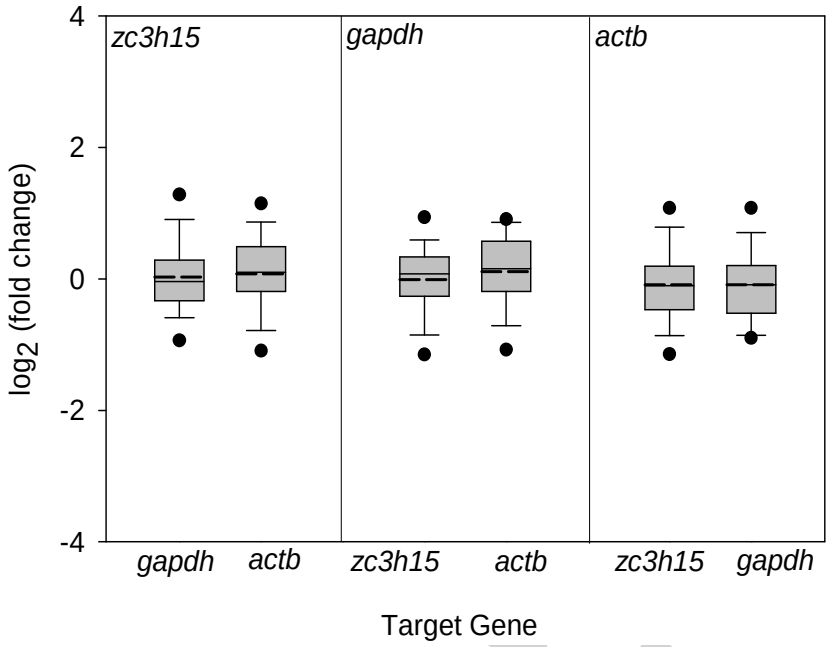

Figure S4. Qualitative analysis of the expression stability of our chosen reference genes (*Z3h15, Gapdh, and Actb*) within our experimental paradigm. The boxplot represents the expression of each reference gene relative to one another, and permits the qualitative evaluation of the relative expression variability of the reference genes upon incubation of rat ovary with GNPs (n=96 rats). Variability in reference gene expression was observed across all experimental groups. The *solid line* represents the median and the *dashed* line represents the mean of each respective data set. Each *box* represents the 50^{th} (25^{th}/75^{th}) percentile and each set of *whiskers* represents the 90^{th} (5^{th}/95^{th}) percentile.

Table S5. Summary of simple linear regression analyses of *E2 Accumulation* (y-variable) as a function of each target gene (x-variable).

X	b (estimate)	SE	F	r^2	adj r^2	p-value
Cyp19a1	0.0829	0.676	1.505	0.0217	0.00727	0.224
Star	0.21	0.176	1.431	0.0206	0.00621	0.236
Cyp11a1	0.104	0.119	0.766	0.0111	0.00	0.385
Sod2	0.184	0.14	1.733	0.0249	0.0105	0.192
Hmox1	0.088	0.134	0.431	0.00629	0.00	0.514
Hsd3b1	**0.508**	**0.167**	**9.268**	**0.12**	**0.107**	**0.003**
Cyp17a1	**0.271**	**0.956**	**8.012**	**0.105**	**0.0922**	**0.006**

Data were pooled for each of these analyses without regard for incubation period or gold nanoparticle concentration. Bold text = statistically significant relationship ($p<0.05$).

Table S6. Summary of simple linear regression analyses of *P4 Accumulation* (y-variable) as a function of each target gene (x-variable).

X	b (estimate)	SE	F	r^2	adj r^2	p-value
Hsd3b1	0.500	0.273	3.341	0.039	0.0278	0.071
Sod2	0.0109	0.248	0.00193	0.0000238	0.000	0.965
Hmox1	0.028	0.228	0.015	0.000186	0.000	0.903
Star	**0.884**	**0.314**	**7.925**	**0.0891**	**0.0779**	**0.006**
Cyp11a1	**0.447**	**0.205**	**4.747**	**0.0554**	**0.0437**	**0.032**

Data were pooled for each of the analyses without regard for incubation period or GNP concentration. Bold text = statistically significant relationship ($p<0.05$).

Table S7. Summary of multiple-regression analyses of E2 accumulation (y-variable) as a function of *Cyp19a1*, *Star*, *Cyp11a1*, *Sod2*, and *Hmox1* with concurrent consideration of time and concentration (x-variables).

X	b (estimate)	SE	p-value (variable)	F	r^2	adj r^2	p-value (Model)
Cyp19a1	0.0783	0.069	0.261	0.634	0.0280	0.000	0.596
Time	-0.00095	0.00739	0.898				
concentration	-0.0301	0.0465	0.52				
Star	0.201	0.182	0.273	0.613	0.0271	0.000	0.609
time	-0.00178	0.00748	0.812				
concentration	-0.029	0.0467	0.537				
Cyp11a1	0.111	0.124	0.376	0.468	0.0208	0.021	0.705
time	-0.00204	0.00762	0.79				
concentration	-0.0353	0.0464	0.443				
Sod2	0.18	0.148	0.228	0.556	0.0308	0.031	0.556
time	-0.00251	0.00756	0.741				
concentration	-0.0252	0.047	0.594				
Hmox1	0.0903	0.139	0.518	0.343	0.0154	0.015	0.794
time	-0.00148	0.00760	0.847				
concentration	-0.0354	0.0465	0.45				

Data were pooled for each of the analyses without regard for incubation period or gold nanoparticle concentration. None of these multiple-regression models showed a statistically significant relationship between E2 accumulation and the independent variables included in these analyses.

Table S8. Summary of multiple-regression analyses of E2 accumulation (y-variable) as a function of *Hsd3b1*, *Cyp17a1*, time and concentration (x-variables).

X	b (estimate)	SE	p-value (variable)	F	r^2	adj r^2	p-value (Model)
Hsd3b1	0.511	0.177	***0.005***	3.011	0.12	0.080	0.036
time	-0.00125	0.00702	0.860				
concentration	-0.00167	0.0459	0.971				
Cyp17a1	0.307	0.099	***0.003***	3.442	0.135	0.960	0.022
time	-0.00503	0.00711	0.482				
concentration	-0.0612	0.443	0.172				
Cyp17a1	0.267	0.0898	***0.004***	9.594	0.223	0.199	<0.001
Hsd3b1	-0.502	0.158	***0.002***				
Hsd3b1	0.481	0.167	***0.005***	4.955	0.187	0.002	0.002
Cy17a1	-0.292	0.0941	***0.003***				
time	-0.00557	0.00675	0.412				
concentration	0.0243	0.044	0.582				

Data were pooled for each of the analyses without regard for incubation period or gold nanoparticle concentration. All multiple-regression models presented here showed statistical significance ($p<0.05$). Bold text is indicative of the predictor variable(s) derived from each respective regression model.

Table S9. Summary of multiple-regression analyses of P4 accumulation (y-variable) as a function of each target gene, time, or concentration (x-variables).

X	b (estimate)	SE	p-value (variable)	F	r^2	adj r^2	p-value (Model)
Hsd3b1	0.484	0.277	0.085	1.529	0.057	0.0212	0.198
time	0.0145	0.0127	0.257				
concentration	0.0365	0.0815	0.655				
Sod2	0.0952	0.256	0.711	0.601	0.0223	0.000	0.616
time	0.0154	0.0132	0.246				
concentration	0.0629	0.0834	0.453				
Hmox1	0.0154	0.229	0.947	0.555	0.0207	0.000	0.646
time	0.0144	0.270	0.270				
concentration	0.0575	0.486	0.486				
Cyp11a1	0.404	0.214	0.063	1.761	0.0627	0.0271	0.161
time	0.008822	0.013	0.499				
concentration	0.0365	0.0811	0.654				
Star	**0.837**	**0.321**	**0.011**	**2.868**	**0.0982**	**0.064**	**0.042**
time	0.0095	0.0126	0.451				
concentration	0.0411	0.0791	0.605				
Star	**0.787**	**0.315**	**0.014**	**5.651**	**0.124**	**0.102**	**0.005**
Cyp11a1	0.359	0.202	0.079				
Star	**0.767**	**0.321**	**0.019**	**2.826**	**0.127**	**0.0818**	**0.030**
Cyp11a1	0.335	0.21	0.115				
time	0.00524	0.0054	0.681				
concentration	0.0251	0.0251	0.751				

Data were pooled for each of the analyses without regard for incubation period or gold nanoparticle concentration. Bold text is indicative of the predictor variable(s) derived from each statistically significant regression model ($p<0.05$).

Table S10. Summary of concentration-specific regression analyses of E2 accumulation (y-variable) as a function of *Cyp17a1*, *Hsd3b1*, or time (x-variables).

Regression	Concentration	X	b (estimate)	SE	p-value (variable)	F	r^2	adj r^2	p-value (Model)
Simple	$1.43x10^3$	*Cyp17a1*	0.0931	0.163		0.328	0.0147	0.000	0.572
Simple	$1.43x10^6$	*Cyp17a1*	0.365	0.201		3.293	0.136	0.0944	0.084
Simple	**$1.43x10^9$**	***Cyp17a1***	**0.469**	**0.156**		**9.034**	**0.301**	**0.268**	**0.007**
Multiple	**$1.43x10^9$**	***Cyp17a1***	**0.526**	**0.175**	**0.007**	**4.704**	**0.32**	**0.252**	**0.021**
		time	**-0.0094**	**0.0125**	**0.462**				
Simple	**$1.43x10^3$**	***Hsd3b1***	**0.489**	**0.222**		**4.861**	**0.181**	**0.144**	**0.038**
Simple	$1.43x10^6$	*Hsd3b1*	0.54	0.389		1.932	0.0843	0.0407	0.179
Simple	$1.43x10^9$	*Hsd3b1*	0.583	0.396		2.166	0.0935	0.0504	0.156
Multiple	$1.43x10^3$	*Hsd3b1*	0.489	0.227	0.043	2.325	0.181	0.103	0.122
		time	-0.00104	0.0117	0.93				

Units of concentration = particles/mL. Bold text = statistically significant relationship ($p<0.05$).

Table S11. Summary of concentration-specific regression analyses of P4 accumulation (y-variable) as a function of *Star*, *Cyp11a1*, or time (x-variables).

Regression	Concentration	X	b (estimate)	SE	p-value (variable)	F	r^2	adj r^2	p-value (Model)
Simple	$1.43x10^3$	*Star*	0.499	0.348		2.06	0.0893	0.0459	0.166
Simple	**$1.43x10^6$**	***Star***	**2.229**	**0.679**		**10.771**	**0.278**	**0.252**	**0.003**
Simple	$1.43x10^9$	*Star*	0.0524	0.370		0.02	0.000715	0.000	0.888
Multiple	**$1.43x10^6$**	***Star***	**2.253**	**0.793**	**0.008**	**5.196**	**0.278**	**0.224**	**0.012**
		time	**0.00189**	**0.0307**	**0.952**				
Simple	$1.43x10^3$	*Cyp11a1*	0.016	0.155		0.0106	0.000505	0.000	0.919
Simple	**$1.43x10^6$**	***Cyp11a1***	**1.969**	**0.489**		**16.189**	**0.366**	**0.344**	**<0.001**
Simple	$1.43x10^9$	*Cyp11a1*	0.0556	0.287		0.376	0.00134	0.000	0.848
Multiple	**$1.43x10^6$**	***Cyp11a1***	**1.889**	**0.494**	**<0.001**		**0.392**	**0.347**	**0.001**
		time	**0.0264**	**0.0249**	**0.299**				
Multiple	**$1.43x10^6$**	***Star***	**1.292**	**0.783**	**0.111**	**7.075**	**0.449**	**0.386**	**0.001**
		Cyp11a1	**1.511**	**0.0274**	**0.009**				
		time	**0.00475**	**0.0274**	**0.864**				

Units of concentration = particles/mL. Bold text = statistically significant.